Petroleum Science 21 (2024) 2839–2848

Contents lists available at ScienceDirect

Petroleum Science

journal homepage: www.keaipublishing.com/en/journals/petroleum-science

Original Paper

Probing the interaction between asphaltene-wax and its effects on the crystallization behavior of waxes in heavy oil via molecular dynamics simulation

Yong Hu [a], Xi Lu [a], Hai-Bo Wang [a, *], Ji-Chao Fang [a], Yi-Ning Wu [b, **], JianFang Sun [a]

[a] SINOPEC Petroleum Exploration and Production Research Institute, Beijing, 102206, China
[b] Shandong Key Laboratory of Oilfield Chemistry, School of Petroleum Engineering, China University of Petroleum (East China), Qingdao, 266580, Shandong, China

ARTICLE INFO

Article history:
Received 18 October 2023
Received in revised form
30 November 2023
Accepted 7 January 2024
Available online 19 January 2024

Edited by Min Li

Keywords:
Heavy oil
Interaction mechanism
Asphaltenes
Waxes
Molecular dynamics

ABSTRACT

High content of asphaltenes and waxes leads to the high pour point and the poor flowability of heavy oil, which is adverse to its efficient development and its transportation in pipe. Understanding the interaction mechanism between asphaltene-wax is crucial to solve these problems, but it is still unclear. In this paper, molecular dynamics simulation was used to investigate the interaction between asphaltene-wax and its effects on the crystallization behavior of waxes in heavy oil. Results show that molecules in pure wax are arranged in a paralleled geometry. But wax molecules in heavy oil, which are close to the surface of asphaltene aggregates, are bent and arranged irregularly. When the mass fraction of asphaltenes in asphaltene-wax system (ω_{asp}) is 0–25 wt%, the attraction among wax molecules decreases and the bend degree of wax molecules increases with the increase of ω_{asp}. The ω_{asp} increases from 0 to 25 wt %, and the attraction between asphaltene-wax is stronger than that among waxes. This causes that the wax precipitation point changes from 353 to 333 K. While the ω_{asp} increases to 50 wt%, wax molecules are more dispersed owing to the steric hindrance of asphaltene aggregates, and the interaction among wax molecules transforms from attraction to repulsion. It causes that the ordered crystal structure of waxes can't be formed at normal temperature. Simultaneously, the asphaltene, with the higher molecular weight or the more hetero atoms, has more obvious inhibition to the formation of wax crystals. Besides, resins also have an obvious inhibition on the wax crystal due to the formation of asphaltene-resin aggregates with a larger radius. Our results reveal the interaction mechanism between asphaltene-wax, and provide useful guidelines for the development of heavy oil.

1. Introduction

The rapid industrial development causes the global energy demand to constantly increase, but light crude oil resources are decreasing sharply (Wang et al., 2017; Ahmadi et al., 2020; Meyer et al., 2007; Zhao et al., 2022). Simultaneously, heavy oil is becoming an alternative resource due to the wide distribution and abundant reserves. The reserves of heavy oil, ultra-heavy oil, and native bitumen are about 1×10^{12} t worldwide (Yu, 2001; Guo and Zhang, 2014). Compared with light crude oil, higher content of asphaltenes and waxes in heavy oil is identified (Guo et al., 2016; Xu et al., 2021; Dong et al., 2009; Liu et al., 2006; Zhao et al., 2023), which leads to the poor flowability of heavy oil in pit shaft and seriously restricts the development of heavy oil (Su et al., 2019; Ghanavati et al., 2013; Argillier et al., 2002; Luo and Gu, 2005; Huang et al., 2021). The investigation of the interaction between asphaltenes and waxes and its effects on the crystallization behavior of waxes is quite crucial for achieving the economic and effective development of heavy oil.

The effect of asphaltenes on the crystallization behavior of waxes has been widely studied in recent years (Passade-Boupat et al., 2018; Lashkarbolooki et al., 2011; Taheri-Shakib et al., 2020a, 2020b; Li et al., 2019). Xue et al. (2019) investigated the

* Corresponding author.
** Corresponding author.
E-mail addresses: wanghaibo.syky@sinopec.com (H.-B. Wang), wuyining@126.com (Y.-N. Wu).

https://doi.org/10.1016/j.petsci.2024.01.006

effect of asphaltenes and resins on the pour point of waxy oil. They found that asphaltenes and resins could reduce wax precipitation temperature, wax precipitation amount, gelation temperature, and yield stress of waxy oils. Jahnke et al. (2007) and Venkatesan et al. (2003) explored the effect of asphaltenes on the crystal structure of waxes. It was found that the crystal structure of waxes changes from a rod-shaped structure to an elliptical structure with the effect of asphaltenes. Wang et al. (2023) also discussed the effect of asphaltenes on the self-crystallization behavior of waxes. The research results show that asphaltenes can promote the formation of the three-dimensional network structure of waxes and increase the size of wax crystal clusters. The above studies show that asphaltenes have a significant effect on the crystallization behavior of waxes. However, it is unknown that the mechanism of asphaltenes changing the crystallization behavior of waxes.

Currently, there are four main proposals: co-crystal theory (Alcazar-Vara et al., 2012), nucleation (García and Carbognani, 2001; García, 2000; Lei et al., 2016), adsorption (Jahnke et al., 2007), and steric hindrance (Alcazar-Vara and Buenrostro-Gonzalez, 2012). Alcazar-Vara et al. (2012) reported that the wax precipitation point in waxy oil was reduced by the co-crystal which is formed by the alkyl side chains of asphaltene molecules and wax molecules. García and Carbognani (2001, García, 2000) and Lei et al. (2016) proposed that asphaltene aggregates could act as the crystal nuclei to affect the crystallization behavior of waxes, and the aggregation behavior of asphaltenes would be influenced by the three-dimensional network structure of waxes. Jahnke et al. (2007) found that asphaltenes adsorbed on the surface of wax crystals can inhibit the growth of wax crystals. Alcazar-Vara and Buenrostro-Gonzalez (2012) indicated that asphaltenes (with high aromaticity) hindered the interaction between asphaltenes and waxes, then a bigger solubility of waxes and a lower wax precipitation point would be induced. But Lei et al. (2016) considered that the impact of the steric hindrance of asphaltenes on the crystallization behavior of waxes could be ignored. The interaction mechanism between asphaltene-wax is still controversial until now and further research is essential.

In this work, molecular dynamics simulation was used to investigate the interaction between asphaltene-wax and its effects on the crystallization behavior of waxes in heavy oil. The effects of the asphaltene content and the asphaltene molecular structure on the crystallization behavior of waxes were investigated in detail. In addition, the effect of resins on the interaction between asphaltene-wax was also considered. This work clarifies the interaction mechanism between asphaltene-wax in heavy oil at the molecular level. The results can provide the theoretical guidance for the molecular design of pour inhibitors and the efficient development of heavy oil.

2. Simulation method

2.1. Force field and simulation model

Molecular dynamics simulation was carried out using OPLS-AA force field (Ambrose et al., 2012; Jorgensen et al., 1996) via GROMACS-4.6.7 software package (Frenkel and Smit, 1996; Griebel et al., 2010). The force field has been widely applied to research the organic substance. A cubic box with periodic boundary conditions in the XYZ direction was constructed. Waxes (tetracontane), saturates (n-heptane and n-octane), aromatics (p-xylene, o-xylene, m-xylene, and naphthalene), resins (resin 1–5) and asphaltenes (asphaltene 1–3) were used to construct different systems. The specific molecular structure is shown in Fig. 1.

2.2. Simulation process and parameter

The Packmol software (Martínez and Martínez, 2003, 2009) was used to construct the simulation systems and the detailed molecular components of different systems were described in Section 3. The molecular dynamics simulation process mainly included the energy minimization, the simulation under NPT and the simulation under NVT.

Firstly, The energy minimization of simulation systems was carried out via the steepest descent method to obtain the reasonable Initial configurations. The system was considered reasonable until the maximum energy of the system was below 100 kJ/mol. The cut-off was 1.0 nm and the long range electrostatic interactions was treated by PME. Then a 10 ns NPT simulation was performed to scale the volume of the system. During the NPT simulation, the Berendsen method was used to control temperature (293 K) and pressure (1 bar). The time step was 2 fs and the cut-off was 1.4 nm. Finally, a 100 ns NVT simulation was carried out at 293 K to obtain the balanced systems. The Berendsen method was used to control temperature, the time step was 2 fs, and the cut-off was 1.4 nm.

3. Results and discussion

3.1. Asphaltene-wax interaction in heavy oil system

The pure wax system (System 1) and the heavy oil system (System 2) were first constructed to compare the crystallization behavior of waxes in System 1 and System 2. System 1 was built only containing 60 wax molecules. System 2 included saturates, aromatics, resins, asphaltenes, and waxes with the same mass ratio (see Table 1).

The crystallization behavior of waxes in System 1 and System 2 was researched via a 100 ns NVT simulation. The end-to-end distance (EED) refers to the distance between the first and the last atom in the same carbon chain (Rubio et al., 1991). The radius of gyration (R_g) indicates the distance from the center of the differential mass of a molecule to the rotation axis (Affholter et al., 1994; Migliardo et al., 2003). Here, the crystal structure of waxes was analyzed using EED and R_g in System 1 and System 2. Fig. 2(a)–(b) indicate thermodynamically stable geometries for System 1 and System 2, respectively.

Carbon chains of wax molecules are straight in the final structure of System 1, and are arranged in a paralleled geometry (see Fig. 2(a)). By comparison, carbon chains of some wax molecules in System 2 were bent to different extents (see Fig. 2(b)). In System 2, the wax molecules, which are close to the surface of asphaltene aggregates, are evidently bent. The other wax molecules avoiding asphaltene aggregates remain straight. As shown in Fig. 2(c), the EED of System 2 is 3.74 nm, which is less than 4.54 nm of System 1. And the R_g of System 2 is 1.22 nm, which is also less than 1.39 nm of System 1 (see Fig. 2(d)). This indicates that asphaltene aggregates cause a hindrance to affect the ordered arrangement of wax molecules and to inhibit the formation of wax crystals.

Mean square displacement (MSD) refers to the deviation of the molecular space position in the simulation system at a specific time, and the diffusion coefficient (D) of particles is proportional to MSD, and the specific formula is as follows (Allen and Tildesley, 2017; Zhang et al., 2022):

$$\mathrm{MSD} = 2dDt \tag{1}$$

where d is the dimensionality of space. MSD of waxes with the simulation time in System 1 and System 2 is plotted in Fig. 3. MSD of waxes is used to calculate the diffusion coefficient of waxes. The results show that the diffusion coefficient of waxes in System 2 is

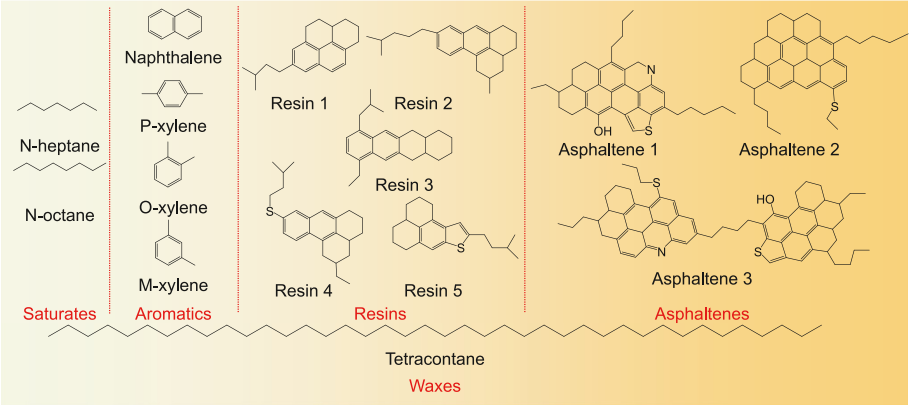

Fig. 1. Molecular structure of waxes, saturates, aromatics, resins and asphaltenes (Song et al., 2018).

Table 1
Molecular components of System 2 and System 2'

Component	Molecule	System 2	System 2′
Saturates	N-heptane	160	160
	N-octane	160	160
Aromatics	P-xylene	77	77
	O-xylene	77	77
	M-xylene	77	77
	Naphthalene	77	77
Resins	Resin 1	22	22
	Resin 2	23	23
	Resin 3	23	23
	Resin 4	23	23
	Resin 5	23	23
Asphaltenes	Asphaltene 1	16	16
	Asphaltene 2	18	18
	Asphaltene 3	17	17
Waxes	$C_{40}H_{82}$	60	/

about 20 times more than that in System 1. In System 1, wax molecules form a regular crystal geometry and the interaction among wax molecules is strong. Wax molecules are limited in location and are difficult to diffuse. In contrast, some wax molecules, which are close to asphaltene aggregates, can diffuse following the asphaltene aggregate migration in System 2.

Based on the above analysis, it is concluded that the steric hindrance induced by asphaltene aggregates can make the carbon chains of wax molecules bend and inhibit the formation of wax crystal. It could reduce the wax precipitation point of heavy oil.

Based on the above research, System 2′ was built, which included saturates, aromatics, resins and asphaltenes with an average mass ratio (see Table 1). The aggregate behavior of asphaltenes in System 2′ and System 2 was compared via a 100 ns NVT simulation. The final stable geometries of asphaltenes in System 2' and System 2 were shown in Fig. 4(a)–(b). The radial distribution function (RDF) is a distribution function that gives the probability of finding a particle around the certain particle (Netzloff and Gordon, 2004). It can be used to analyze the aggregation level of asphaltenes in two systems (see Fig. 4(c)).

As RDFs of asphaltene-asphaltene shown, there are four peaks at $r = 0.31$, 0.43, 0.50 and 0.62 nm in two systems (see Fig. 4(c)). Peak values of System 2 is about 1.5 times more than them of System 2'. It means that the aggregation level of asphaltenes is higher by the restriction of wax crystal. Besides, the cluster number of asphaltenes is 7.0 and 6.5 in System 2' and System 2, respectively (see Fig. 5). This indicates an increase in asphaltene molecules of an asphaltene aggregate.

3.2. Effects of asphaltene contents

Systems 3, 4, and 5 were constructed using only waxes and asphaltenes (see Table 2), in order to further investigate the asphaltene-wax interaction. Mass fractions of asphaltenes (ω_{asp}) in the three systems were 10, 25, and 50 wt%, respectively. Then they were calculated using the 50 ns NVT simulation at 293, 313, 333, 353, and 373 K, respectively. The final geometries of different asphaltene-wax systems were shown in Fig. 6. The total energy of

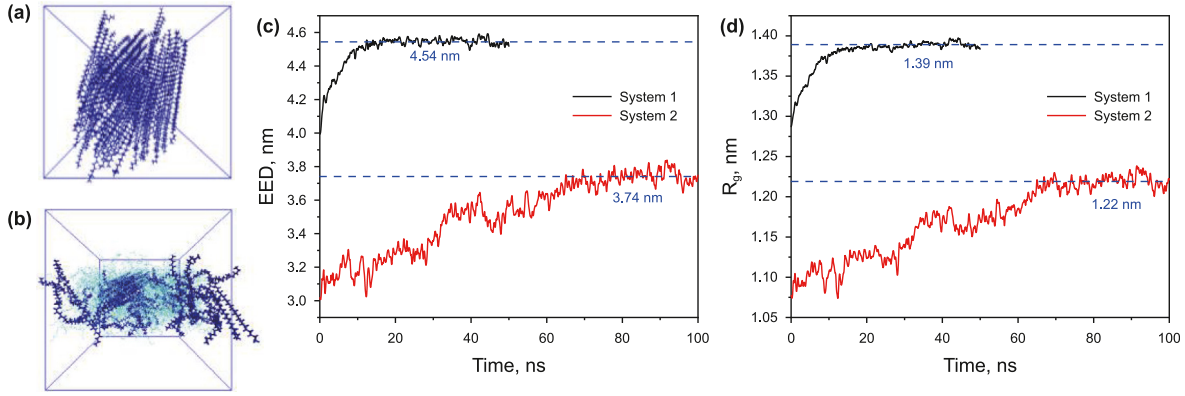

Fig. 2. **(a)** Stable geometry of waxes in System 1; **(b)** stable geometry of waxes in System 2; **(c)** EED of wax molecules in System 1 and System 2; **(d)** R_g of wax molecules in System 1 and System 2.

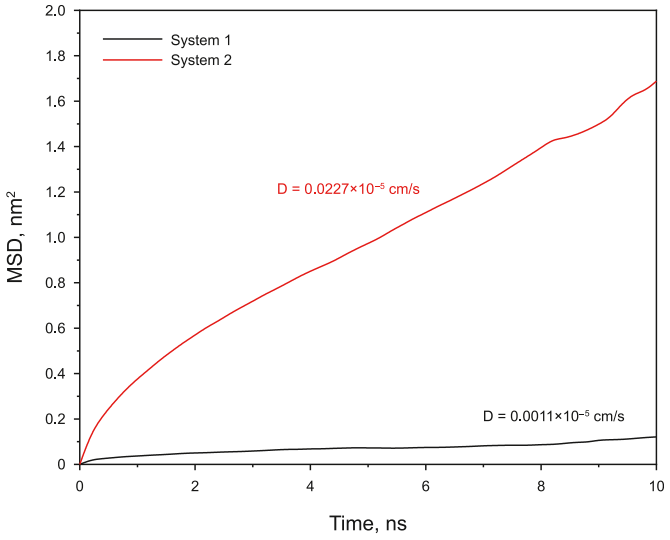

Fig. 3. MSD of wax molecules in System 1 and System 2.

various asphaltene-wax systems was analyzed, and the change of the total energy with temperatures in various asphaltene-wax systems was shown in Fig. 7.

Table 2
Molecular components of systems 3, 4, and 5.

System	Molecule	Molecular number	ω_{asp}, wt%
System 3	Wax	60	90
	Asphaltene 1	2	10
	Asphaltene 2	2	
	Asphaltene 3	2	
System 4	Wax	60	75
	Asphaltene 1	5	25
	Asphaltene 2	6	
	Asphaltene 3	6	
System 5	Wax	60	50
	Asphaltene 1	16	50
	Asphaltene 2	18	
	Asphaltene 3	17	

For System 1 and System 3, the ordered wax crystal transforms to a disordered structure when the temperature is higher than 353 K. The change temperature declined to 333 and 293 K in System 4 and System 5, respectively. It shows that the arrangement of wax molecules tends to become disordered and the change temperature become lower as the ω_{asp} increases. This indicates that the increase of ω_{asp} can inhibit the wax crystal formation. Fig. 7 shows that the total energy increases linearly following the increase of temperature for System 5. But in systems 1, 3 and 4, the total energy grows slowly and then rapidly as temperature increases. The transition temperature of systems 1, 3 and 4 is 353, 353 and 333 K,

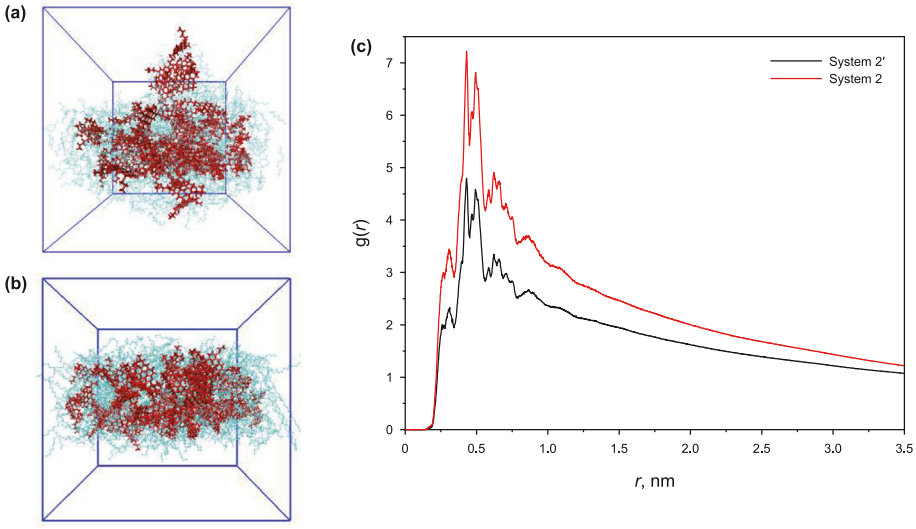

Fig. 4. Final stable geometries of asphaltenes in **(a)** System 2′ and **(b)** System 2; **(c)** RDFs of asphaltene-asphaltene in system 2′ and 2.

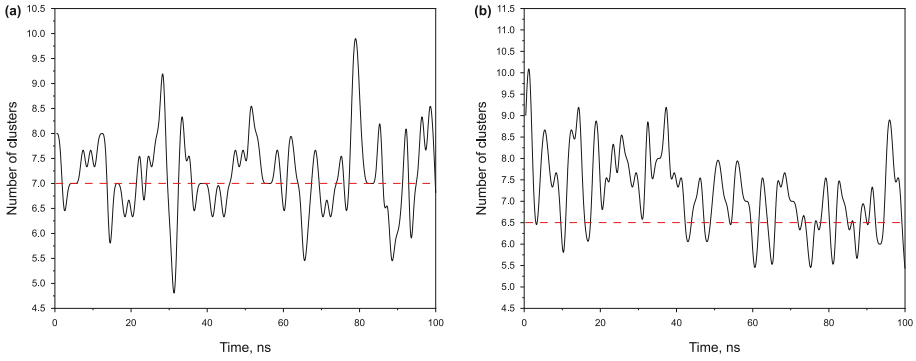

Fig. 5. Cluster number of asphaltene molecules in system 2′ and 2.

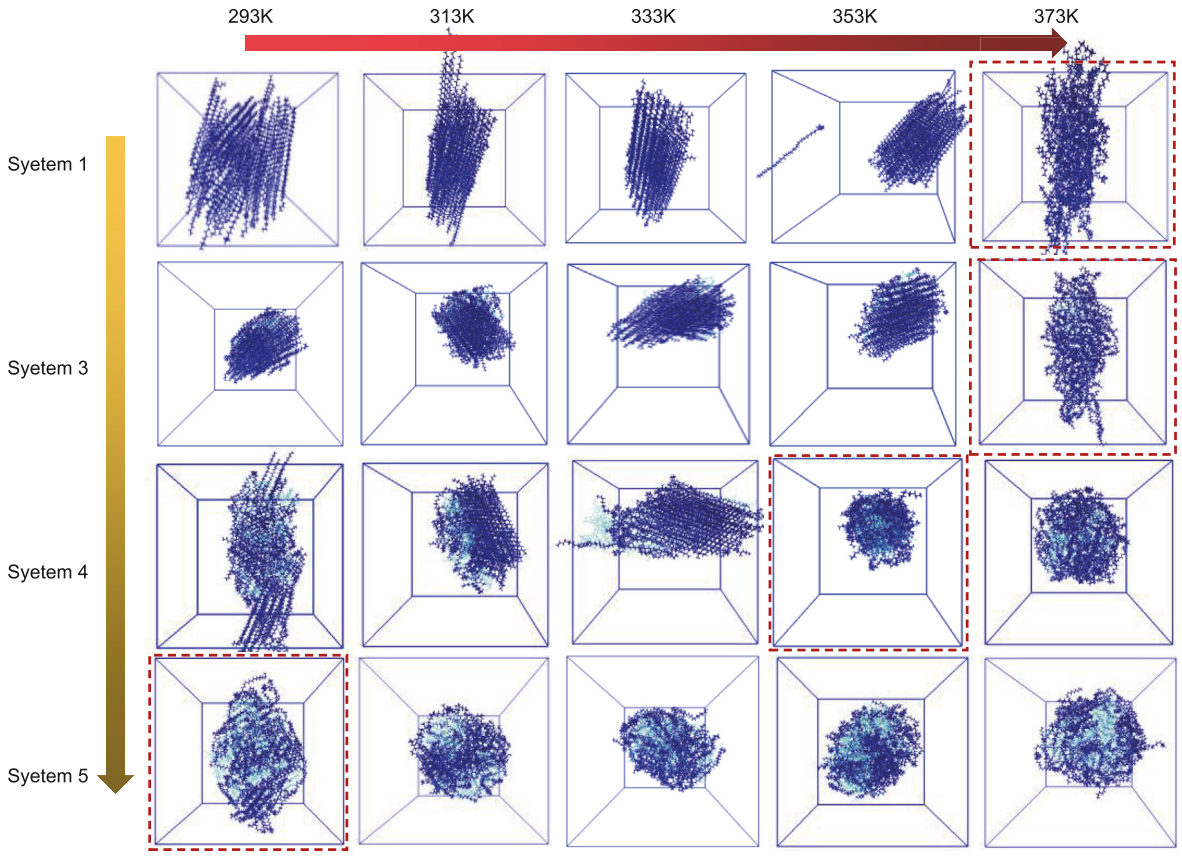

Fig. 6. Final stable geometries of various asphaltene-wax systems.

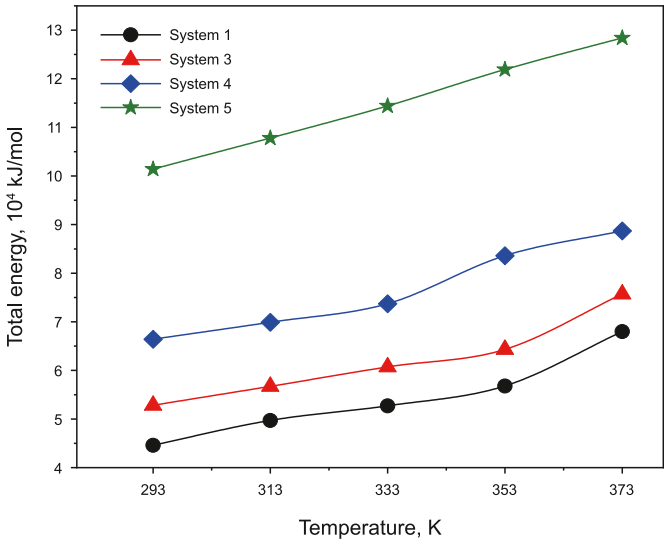

Fig. 7. Change of the total energy over temperatures in asphaltene-wax systems with different asphaltene contents.

respectively. This shows that temperature can lead to the thermodynamical instability of aphaltene-wax systems. Meanwhile, the total energy increase with the increase of ω_{asp} at the same temperature, which indicates the increase of aphaltenes results in the thermodynamical instability of aphaltene-wax systems.

The EED of each wax molecule is analyzed, and the distribution curves of EED are drawn in Fig. 8(a)–(d). The weighted mean value of EED (A_{EED}) can be calculated as:

$$A_{EED} = \sum_{i}^{10} EED_i \times \frac{n_i}{N} \quad (2)$$

where A_{EED} is the weighted mean value of EED of wax molecules in one certain system. EED of wax molecules is in the range of 0–5 nm, and it is divided into 10 segments at the interval of 0.5 nm. EED_i is the mid value of EED in i segment ($i = 1, 2, 3, \ldots, 10$), n_i is the number of wax molecules in i segment ($i = 1, 2, 3, \ldots, 10$), and N is the total number of wax molecules in one certain system. The change of A_{EED} with temperature in various asphaltene-wax systems was shown in Fig. 8(e).

The ranges of A_{EED} of waxes in regular and irregular crystal structures are 4–5 nm and 2–4 nm, respectively (see Figs. 6 and 8(a)–(d)). As shown in Fig. 8(e), A_{EED} of waxes slowly increases at first and then drops to a low value following the increase of temperature for systems 1, 3 and 4. By contraries, A_{EED} of waxes is in the range of 2.75–3.00 nm in System 5. There isn't an evident change in A_{EED} of waxes as the increase of temperature. It is because the arrangement of wax molecules is irregular and the wax crystal can't be formed at 293–373 K in System 5. This indicates that the high asphaltene content can affect the crystallization behavior of waxes. When the ω_{asp} is lower than 25 wt%, asphaltenes don't have an obvious inhibition on the formation of wax crystals and the wax precipitation point is 353 K. Once the ω_{asp} reaches 25 wt%, the wax precipitation point decreases to 333 K. While the ω_{asp} increases to 50 wt%, the ordered wax crystal can't be formed at normal temperature (293 K).

Fig. 9(a) shows that the interaction energy among wax

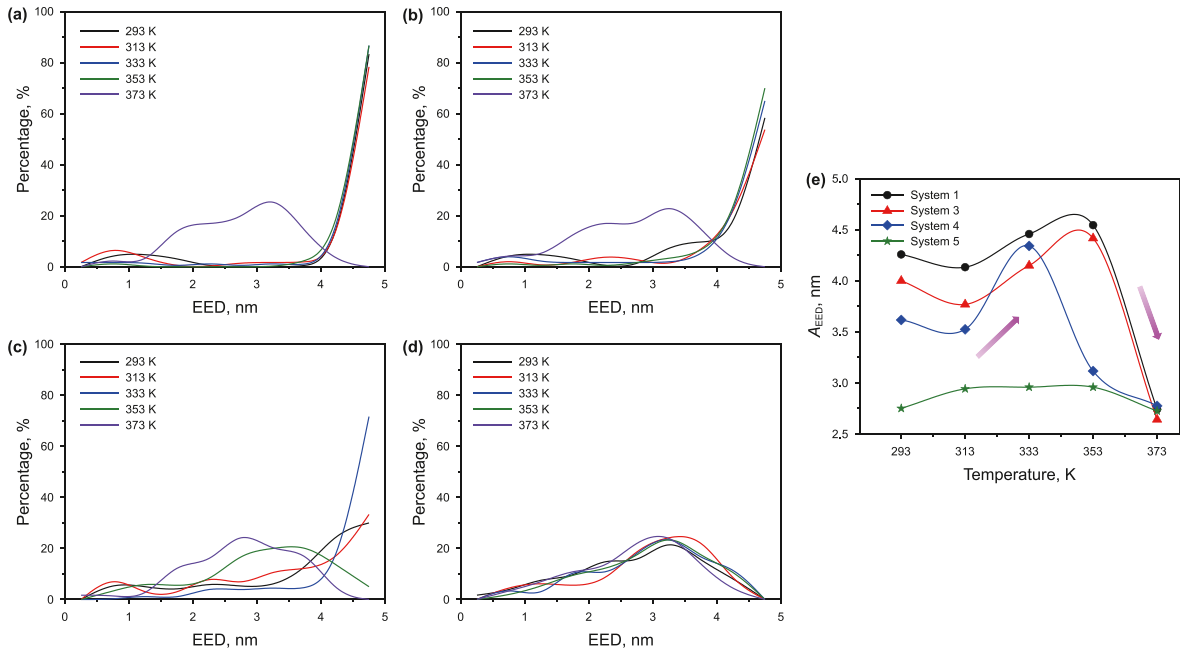

Fig. 8. Distribution curves of EED in **(a)** System 1, **(b)** System 3, **(c)** System 4 and **(d)** System 5; **(e)** change of A_{EED} of waxes with temperature in systems 1, 3, 4, and 5.

molecules changes with the increasing temperature in systems 1, 3, 4, and 5. The interaction energy among wax molecules of systems 1, 3, and 4 is below −500 kJ/mol, which presents an attraction among wax molecules. Moreover, the attraction keeps rising as temperature increases. However, the interaction energy among wax molecules of System 5 is more than 500 kJ/mol, which indicates a repulsion among wax molecules. This repulsion is basically not influenced by temperature. Fig. 9(b) shows the change of the interaction energy between asphaltenes and waxes versus temperature in systems 3, 4, and 5. It presents that the effect of temperature on the interaction between asphaltenes and waxes becomes greater with the increase of ω_{asp}. The thermal motion of asphaltene molecules is more intense as the increase of temperature for one system, which then leads to a higher system enthalpy. The ω_{asp} is higher, the temperature effect is greater. The electrostatic interaction energy and the van der Waals interaction energy between asphaltenes and waxes are calculated (see Table 3). This result shows that the interaction between asphaltenes and waxes is mianly dominated by the van der Waals interaction. By comparison, the attraction among wax molecules is stronger than that between asphaltenes and waxes in System 3, so asphaltenes have no obvious effects on the crystallization behavior of waxes. As the ω_{asp} increases, the attraction between asphaltenes and waxes becomes stronger and is stronger than that among wax molecules, which

Table 3
Electrostatic interaction energy and van der Waals interaction energy between asphaltenes and waxes in systems 3, 4 and 5.

System	Temperature, K	$E_{electrostatic}$, kJ/mol	E_{VDW}, kJ/mol	E_{inter}, kJ/mol
System 3	293	15.82	−1259.18	−1243.36
	313	8.93	−1640.75	−1631.82
	333	1.64	−1379.24	−1377.60
	353	12.92	−1432.42	−1419.50
	373	45.20	−1317.26	−1272.06
System 4	293	69.51	−4511.82	−4442.31
	313	52.53	−4260.99	−4208.46
	333	42.20	−3159.96	−3117.76
	353	96.19	−3627.18	−3530.99
	373	103.59	−3701.03	−3597.45
System 5	293	160.50	−9488.59	−9328.09
	313	87.51	−8937.91	−8850.40
	333	196.01	−9335.30	−9139.29
	353	189.48	−8182.74	−7993.26
	373	191.14	−7437.25	−7246.11

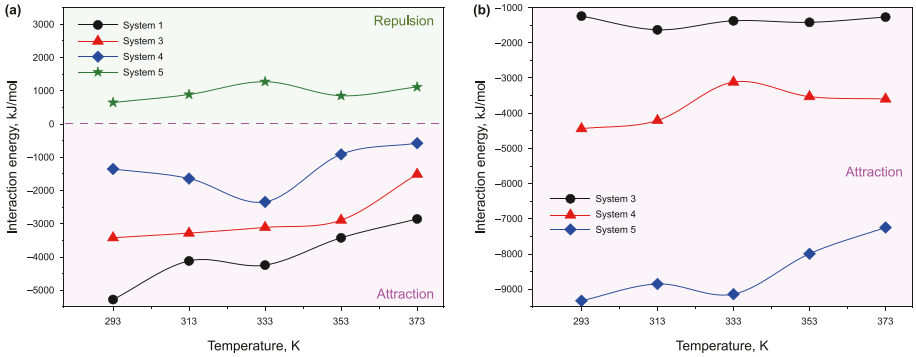

Fig. 9. **(a)** Change of the interaction energy among wax molecules versus temperature in asphaltene-wax systems; **(b)** change of the interaction energy between asphaltenes and waxes versus temperature in asphaltene-wax systems.

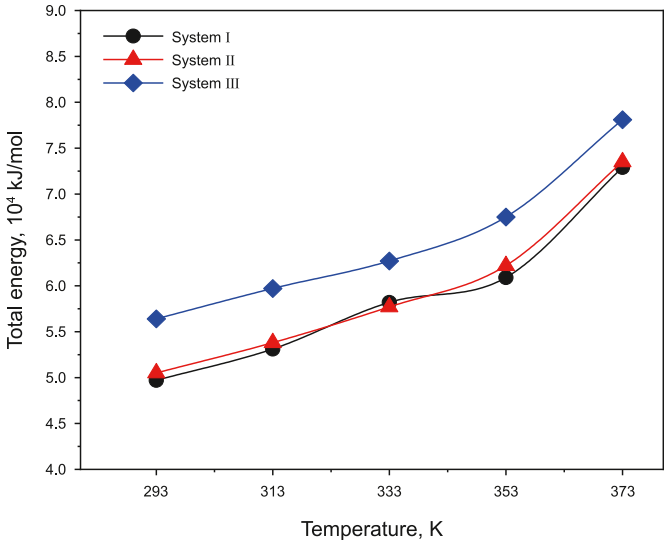

Fig. 10. Change of the total energy over temperatures in wax-asphaltene systems with different asphaltenes.

lead to the change of the wax crystallization and the reduction of the wax precipitation point.

3.3. Influences of the asphaltene geometry

As known, heavy oil is a complicated mixture consisting of different chemical components. Thus, asphaltenes contain various molecular geometries, which affect the interaction between asphaltenes and waxes. Asphaltene-wax systems I, II, and III were established using asphaltene 1, 2, and 3, respectively. Comparing asphaltene 1 with 2, asphaltene 1 has more heteroatoms. Comparing asphaltene 1 with 3, asphaltene 3 has the higher molecular weight and the larger steric hindrance. The molecular dynamics simulation was performed under NVT ensemble at 293, 313, 333, 353 and 373 K, respectively. The change of the total energy with temperature in various asphaltene-wax systems was shown in Fig. 10.

Fig. 10 shows that the change curves of the total energy over temperatures in System I and System II are almost overlapped. Compared with the two systems, the total energy of system III is higher. This illuminates that asphaltene 3 has the greater effect on the thermodynamical instability of aspaltene-wax systems and the crystallization behavior of waxes.

Fig. 11(a)–(c) show the distribution curves of EED of wax molecules in systems I, II and III under different temperatures, respectively. EED of wax molecules ranges from 4 to 5 nm at 293–353 K and is in the range of 2–4 nm at 373 K in three systems. The final computed configuration at 373 K is also presented in Fig. 11(a)–(c), respectively. Carbon chains of wax molecules are bent or twisted to some extent and the arrangement of wax molecules becomes disordered at 373 K in three configurations. The change of A_{EED} of waxes is similar to a para curve as the increasing temperature in three systems (see Fig. 11(d)). All max peak values correspond to 353 K, which indicates the transformation temperature of the wax crystal configuration. A_{EED} of waxes in System I is maximal, and that in System III is minimum. Consequently, the high molecular weight of asphaltenes can benefit the bending or twisting of wax molecules below 353 K. As the temperature rises, the thermos motion makes asphaltenes run away from waxes and

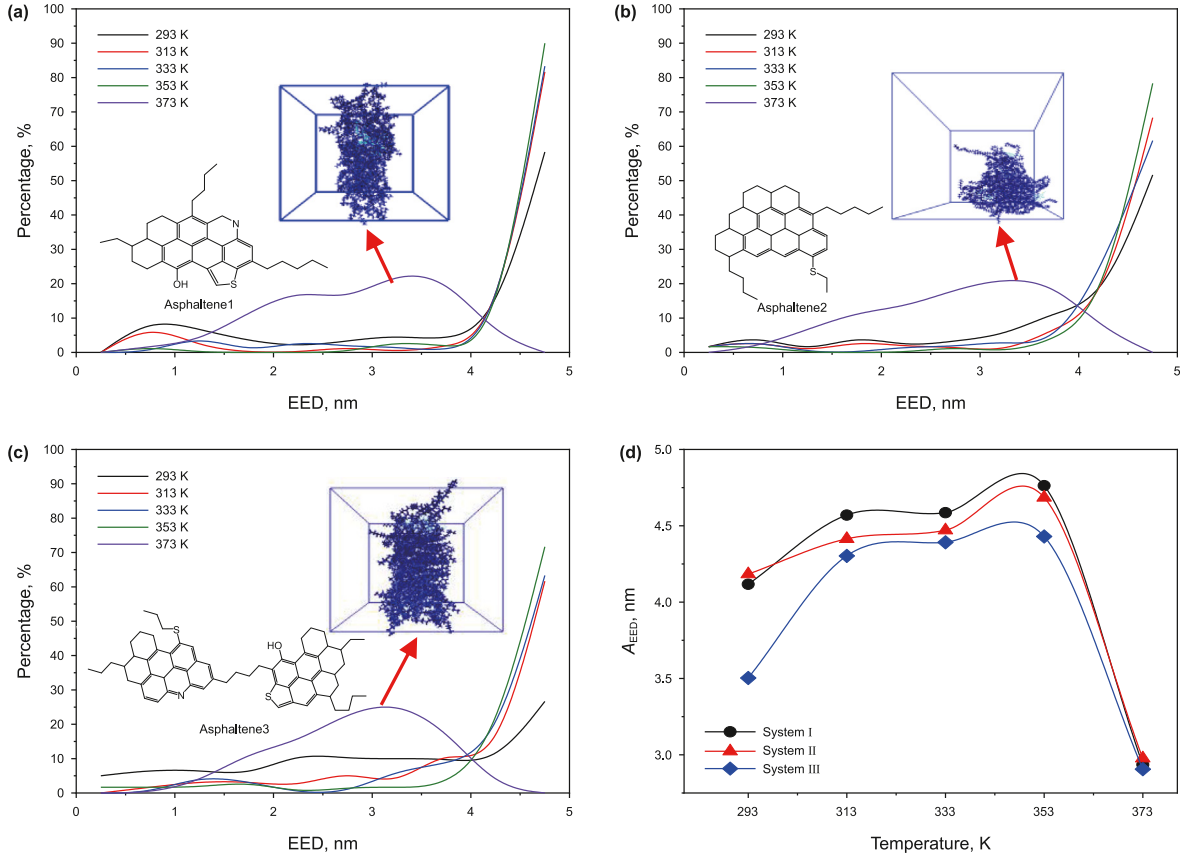

Fig. 11. Distribution curves of EED in **(a)** Systems I, **(b)** System II, and **(c)** System III; **(d)** change of A_{EED} of wax molecules versus temperature in different asphaltene-wax systems.

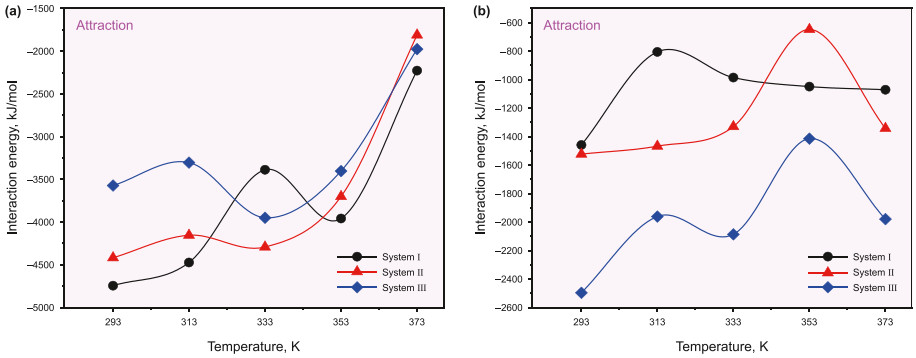

Fig. 12. **(a)** Change of the interaction energy among wax molecules with temperature in different systems; **(b)** change of the interaction energy between asphaltenes and waxes with temperature in different systems.

Table 4
Electrostatic interaction energy and van der Waals interaction energy between asphaltenes and waxes in systems I, II, and III

System	Temperature, K	$E_{electrostatic}$, kJ/mol	E_{VDW}, kJ/mol	E_{inter}, kJ/mol
System I	293	9.93	−1469.08	−1459.15
	313	4.67	−810.71	−806.05
	333	9.30	−995.16	−985.85
	353	8.77	−1057.93	−1049.16
	373	22.81	−1094.22	−1071.41
System II	293	30.30	−1553.10	−1522.80
	313	37.12	−1504.06	−1466.94
	333	37.30	−1367.33	−1330.03
	353	33.88	−682.33	−648.45
	373	40.54	−1382.92	−1342.38
System III	293	42.85	−2538.89	−2496.04
	313	31.99	−1993.41	−1961.42
	333	42.49	−2128.05	−2085.56
	353	32.15	−1446.42	−1414.27
	373	54.11	−2033.05	−1978.94

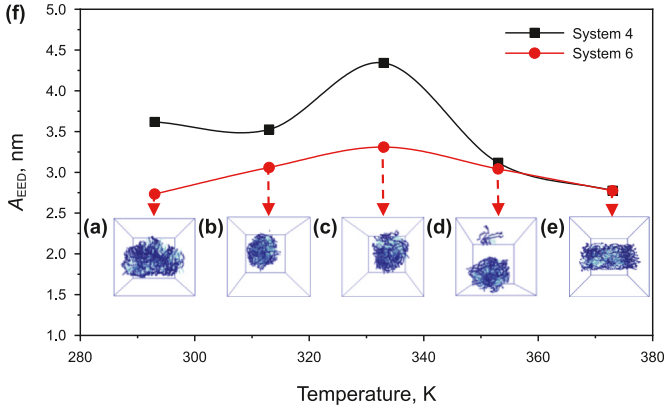

Fig. 13. Final computed configurations of System 6 at **(a)** 293 K, **(b)** 313 K, **(c)** 333 K, **(d)** 353 K, and **(e)** 373 K, respectively; **(f)** change of A_{EED} of wax molecules versus temperature in System 4 and System 6.

reduces the effect of asphaltenes on the arrangement of wax molecules. A_{EED} achieves the similar lowest value at 373 K for three systems, which indicates the influence of the asphaltene geometry on the arrangement of wax molecules nearly disappears at 373 K.

Fig. 12 shows the change in the interaction energy versus temperature. Wax molecules generate a significant attraction to each other in three systems, and it is enhanced when temperature decreases. The attraction of System I is the largest, and that of System III is the lowest at the same temperature (see Fig. 12(a)). On the contrary, the interaction between asphaltenes and waxes of System III is the largest, and that of System I is the lowest (see Fig. 12(b)). As shown in Table 4, the electrostatic interaction between asphaltenes and waxes is repulsive and the van der Waals interaction between asphaltenes and waxes is attractive in the three systems. The van der Waals interaction is much greater than the electrostatic interaction. Comparing asphaltene 1, 2 and 3, the van der Waals interaction between asphaltene 3 and wax is strongest, and the electrostatic interaction between asphaltene 1 and wax is weakest. Thus, asphaltenes with the higher molecular weight or the more hetero atoms can cause a stronger interaction with waxes and have a more obvious inhibition on the formation of wax crystals. However, it induces only a limited influence on the intermolecular interaction among wax molecules.

3.4. Effects of resins

Besides asphaltenes and waxes, resins are generally an important factor contributing to the poor flowability of heavy oil. System 6 consists of 50 wt% waxes, 25 wt% asphaltenes, and 25 wt% resins. Compared with System 4, the influence of resins on the interaction between asphaltenes and waxes is investigated. The molecular dynamic simulation is then carried out at 293, 313, 333, 353, and 373 K, respectively. Final configurations of System 6 at different temperatures are shown in Fig. 13(a)–(e). As the temperature increases, waxes is more dispersive and the asphaltene-resin aggregate becomes more tight.

The change of A_{EED} of wax molecules versus temperature is shown in Fig. 13(f). The two A_{EED} curves have the highest peaks at 333 K, and the temperature is an order-to-disorder transition temperature. A_{EED} of wax molecules in System 4 is in the range of 2.7–4.5 nm. A_{EED} of wax molecules in System 6 ranges from 2.7 to 3.3 nm. It is because resins tightly embrace around asphaltene aggregates to form novel asphaltene-resin aggregates with a larger radius. These aggregates induce a higher steric hindrance and disperse wax molecules, which can decrease the wax precipitation point of heavy oil.

Fig. 14(a) presents the interaction energy among wax molecules in System 4 and System 6. Wax molecules induce an attraction in System 4. As the increase of temperature, the attraction among wax molecules increases before 333 K and then decreases. However, the interaction among wax molecules transforms into a repulsion in System 6 under the influence of resins. The temperature has little impact on the repulsion among wax molecules. As Fig. 14(b) shown, resins only induce a light influence on the asphaltene-wax interaction. In conclusion, resins can further enhance the level of aggregates to influence the arrangement of wax molecules and to reduce the wax precipitation point of heavy oil.

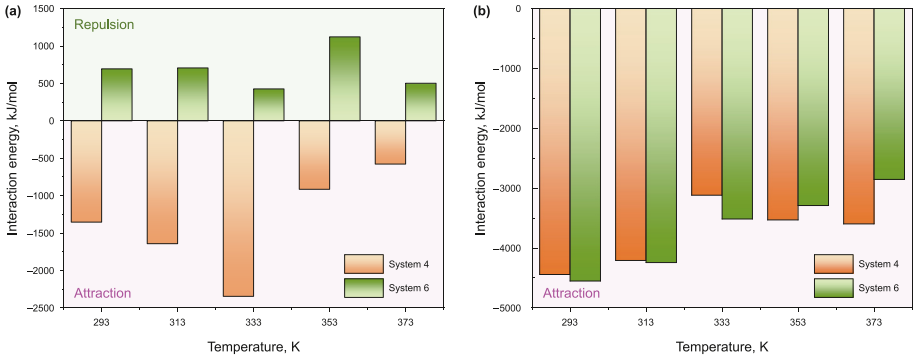

Fig. 14. **(a)** Column charts of the interaction energy among waxes of System 4 and System 6 at different temperatures; **(b)** column charts of the asphaltene-wax interaction energy of System 4 and System 6 at different temperatures.

4. Conclusions

Molecular dynamics simulation is performed to investigate the interaction between asphaltene-wax and its influence on the crystallization behavior of waxes in this study. According to computational results, carbon chains of wax molecules are bent or twisted to some extent due to the attraction between asphaltenes and waxes in heavy oil. The steric hindrance of asphaltene aggregates limits the formation of the wax crystal and reduces the wax precipitation point of heavy oil. When the asphaltene content in asphaltene-wax systems is 0–25 wt%, the attraction among wax molecules decreases as the increasing asphaltene content. But the interaction among wax molecules transforms from attraction to repulsion in the asphaltene-wax system with 50 wt% asphaltenes. It is more difficult to form the ordered wax crystal under the effect of asphaltenes with the higher molecular weight or the more hetero atoms. Moreover, resins can form bigger aggregates with asphaltenes, so the obvious inhibition on the formation of the wax crystal is observed. This work can provide theoretical guidance for the efficient development of heavy oil.

CRediT authorship contribution statement

Yong Hu: Writing – original draft, Methodology, Funding acquisition, Formal analysis, Data curation, Conceptualization. **Xi Lu:** Writing – review & editing, Project administration, Methodology, Investigation. **Hai-Bo Wang:** Writing – review & editing, Project administration, Methodology, Funding acquisition, Conceptualization. **Ji-Chao Fang:** Project administration, Methodology, Investigation, Funding acquisition. **Yi-Ning Wu:** Writing – review & editing, Methodology, Data curation, Conceptualization. **JianFang Sun:** Writing – review & editing, Software, Resources, Project administration, Methodology, Investigation.

Declaration of competing interest

There are no conflicts of interest to declare.

Acknowledgements

This study is financially supported by the Project funded by China Postdoctoral Science Foundation (NO. 2022M723500), the National Natural Science Foundation of China (NO. 52204069) and the Sinopec Science and Technology Project of China (NO. P22015).

References

Affholter, K.A., Henderson, S.J., Wignall, G.D., et al., 1994. ChemInform abstract: structural characterization of C_{60} and C_{70} fullerenes by small-angle neutron scattering. ChemInform. https://doi.org/10.1002/chin.199410001.

Ahmadi, M., Hou, Q., Wang, Y., et al., 2020. Interfacial and molecular interactions between fractions of heavy oil and surfactants in porous media: comprehensive review. Adv. Colloid Interface Sci. 283, 102242. https://www.sciencedirect.com/science/article/pii/S000186862030227X.

Alcazar-Vara, L.A., Buenrostro-Gonzalez, E., 2012. Experimental study of the influence of solvent and asphaltenes on liquid-solid phase behavior of paraffinic model systems by using DSC and FT-IR techniques. J. Therm. Anal. Calorim. 107 (3), 1321–1329. https://doi.org/10.1007/s10973-011-1592-8.

Alcazar-Vara, L.A., Garcia-Martinez, J.A., Buenrostro-Gonzalez, E., 2012. Effect of asphaltenes on equilibrium and rheological properties of waxy model systems. Fuel 93, 200–212. https://doi.org/10.1016/j.fuel.2011.10.038.

Allen, M.P., Tildesley, D.J., 2017. Computer Simulation of Liquids, second ed. Oxford University Press, Oxford. https://doi.org/10.1093/oso/9780198803195.001.0001.

Ambrose, R.J., Hartman, R.C., Diaz-Campos, M., et al., 2012. Shale gas-in-place calculations Part I: new pore-scale considerations. SPE J. 17 (1), 219–229. https://doi.org/10.2118/131772-PA.

Argillier, J.F., Coustet, C., Hénaut, I., 2002. Heavy oil rheology as a function of asphaltene and resin content and temperature. In: SPE International Thermal Operations and Heavy Oil Symposium and International Horizontal Well Technology Conference, 79496. https://doi.org/10.2118/79496-MS. Calgary, Alberta, Canada.

Dong, M., Ma, S., Liu, Q., 2009. Enhanced heavy oil recovery through interfacial instability: a study of chemical flooding for Brintnell heavy oil. Fuel 88, 1049–1056. https://www.sciencedirect.com/science/article/pii/S0016236108004675.

Frenkel, D., Smit, B., 1996. Understanding Molecular Simulation: from Algorithms to Applications, second ed. Academic Press, Amsterdam.

García, M.C., 2000. Crude oil wax crystallization. The effect of heavy n-paraffins and flocculated asphaltenes. Energy Fuel. 14 (5), 1043–1048. https://doi.org/10.1021/ef0000330.

García, M.C., Carbognani, L., 2001. Asphaltene-paraffin structural interactions. Effect on crude oil stability. Energy Fuel. 15 (5), 1021–1027. https://doi.org/10.1021/ef0100303.

Ghanavati, M., Shojaei, M.J., Ahmad Ramazani, S.A., 2013. Effects of asphaltene content and temperature on viscosity of Iranian heavy crude oil: experimental and modeling study. Energy Fuel. 27 (12), 7217–7232. https://doi.org/10.1021/ef400776h.

Griebel, M., Knapek, S., Zumbusch, G., 2010. Numerical Simulation in Molecular Dynamics: Numerics, Algorithms, Parallelization, Applications. Springer Publishing Company, Incorporated, pp. 213–214.

Guo, J., Zhang, J., 2014. Review on the technology of blending diluting oil in heavy oil well. Sci. Technol. Eng. 36 (14), 124–132 (in Chinese).

Guo, K., Li, H., Yu, Z., 2016. In-situ heavy and extra-heavy oil recovery: a review. Fuel 185, 886–902. https://www.sciencedirect.com/science/article/pii/S0016261163078 52.

Huang, Q., Li, H., Zhuang, Y., et al., 2021. Reducing viscosity of waxy crude oil with electric ffeld perpendicular to oil's flow direction. Fuel 283, 119345. https://doi.org/10.1016/j.fuel.2020.119345.

Jahnke, J.P., Tinsley, J.F., Prudhomme, R.K., et al., 2007. Waxy gels with asphaltenes 1: characterization of precipitation, gelation, network strength and morphology. Energy Fuels 23 (4), 2056–2064. https://doi.org/10.1021/ef800636f.

Jorgensen, W.L., Maxwell, D.S., Tirado-Rives, J., 1996. Development and testing of the OPLS all-atom force field on conformational energetics and properties of organic liquids. J. Am. Chem. Soc. 118 (45), 11225–11236. https://doi.org/10.1021/ja9621760.

Lashkarbolooki, M., Esmaeilzadeh, F., Mowla, D., 2011. Mitigation of wax deposition by wax-crystal modifier for Kermanshah crude oil. J. Dispersion Sci. Technol. 32 (7), 975–985. https://doi.org/10.1080/01932691.2010.488514.

Lei, Y., Han, S., Zhang, J., 2016. Effect of the dispersion degree of asphaltene on wax

deposition in crude oil under static conditions. Fuel Process. Technol. 146, 20–28. https://doi.org/10.1016/j.fuproc.2016.02.005.
Li, C., Zhu, H., Yang, F., Liu, H., et al., 2019. Effect of asphaltene polarity on wax precipitation and deposition characteristics of waxy oils. Energy Fuel. 33 (8), 7225–7233. https://doi.org/10.1021/acs.energyfuels.9b01464.
Liu, Q., Dong, M., Yue, X., et al., 2006. Synergy of alkali and surfactant in emulsification of heavy oil in brine. Colloids Surfaces A Physicochem. Eng. Asp. 273, 219–228. https://www.sciencedirect.com/science/article/pii/S092777570500.
Luo, P., Gu, Y., 2005. Effects of asphaltene content and solvent concentration on heavy oil viscosity. In: SPE International Thermal Operations and Heavy Oil Symposium, 97778. https://doi.org/10.2118/97778-MS. Calgary, Alberta, Canada.
Martínez, L., Andrade, R., Birgin, E.G., et al., 2009. PACKMOL: a package for building initial configurations for molecular dynamics simulations. J. Comput. Chem. 30, 2157–2164. https://doi.org/10.1002/jcc.21224.
Martínez, J.M., Martínez, L., 2003. Packing optimization for automated generation of complex system's initial configurations for molecular dynamics and docking. J. Comput. Chem. 24, 819–825. https://doi.org/10.1002/jcc.10216.
Meyer, R., Attanasi, E., Freeman, P., 2007. Heavy oil and natural bitumen resources in geologic basins of the world. Open File Rep. 1084. https://doi.org/10.3133/ofr20071084.
Migliardo, F., Magazù, V., Migliardo, M., 2003. Structural properties of C_{60} in solution. J. Mol. Liq. 110 (1–3), 3–6. https://doi.org/10.1016/j.molliq.2003.08.010.
Netzloff, H.M., Gordon, M.S., 2004. The effective fragment potential: small clusters and radial distribution functions. J. Chem. Phys. 121, 2711–2714. https://doi.org/10.1063/1.1768511.
Passade-Boupat, N., Gingras, J.P., Desplobins, C., et al., 2018. Could the asphaltene solubility class index be used as the “wax appearance temperature” of asphaltenes? Illustration through the study of the polydispersity of PetroPhase 2017 asphaltenes. Energy Fuels 32 (3), 2760–2768. https://doi.org/10.1021/acs.energyfuels.7b02779.
Rubio, A.M., Freire, J.J., Horta, A., et al., 1991. Influence of long-range interactions on the end-to-end distance distribution and cyclization probability of short chains. Macromolecules 24 (18), 5167–5170. https://doi.org/10.1021/ma00018a022.
Song, S., Zhang, H., Sun, L., et al., 2018. Molecular dynamics study on aggregating behavior of asphaltene and resin in emulsified heavy oil droplets with sodium dodecyl sulfate. Energy Fuels 32, 12383–12393. https://doi.org/10.1021/acs.energyfuels.8b03258.
Su, G., Zhang, H., Geng, T., et al., 2019. Effect of SDS on reducing the viscosity of heavy oil: a molecular dynamics study. Energy Fuels 33 (6), 4921–4930. https://doi.org/10.1021/acs.energyfuels.9b00006.
Taheri-Shakib, J., Saadati, N., Esfandiarian, A., et al., 2020a. Characterizing the wax-asphaltene interaction and surface morphology using analytical spectroscopy and microscopy techniques. J. Mol. Liq. 302, 112506. https://doi.org/10.1016/j.molliq.2020.112506.
Taheri-Shakib, J., Zojaji, I., Saadati, N., et al., 2020b. Investigating molecular interaction between wax and asphaltene: accounting for wax appearance temperature and crystallization. J. Pet. Sci. Eng. 191, 107278. https://doi.org/10.1016/j.petrol.2020.107278.
Venkatesan, R., Östlund, J.A., Chawla, H., et al., 2003. The effect of asphaltenes on the gelation of waxy oils. Energy Fuel. 17 (6), 1630–1640. https://doi.org/10.1021/ef034013k.
Wang, C., Gao, L., Liu, M., et al., 2023. Self-crystallization behavior of paraffin and the mechanism study of SiO_2 nanoparticles affecting paraffin crystallization. Chem. Eng. J. 452, 139287. https://doi.org/10.1016/j.cej.2022.139287.
Wang, L., Tian, Y., Yu, X., et al., 2017. Advances in improved/enhanced oil recovery technologies for tight and shale reservoirs. Fuel 210, 425–445. https://doi.org/10.1016/j.fuel.2017.08.095.
Xu, J., Xue, S., Zhang, J., et al., 2021. Molecular design of the amphiphilic polymer as a viscosity reducer for heavy crude oil: from mesoscopic to atomic scale. Energy Fuels 35, 1152–1164. https://doi.org/10.1021/acs.energyfuels.0c03260.7405.
Xue, H., Zhang, J., Han, S., et al., 2019. Effect of asphaltenes on the structure and surface properties of wax crystals in waxy oils. Energy Fuel. 33 (10), 9570–9584. https://doi.org/10.1021/acs.energyfuels.9b01825.
Yu, L., 2001. Distribution of world heavy oil reserves and its recovery technologies and futrue. Special Oil Gas Reservoirs 8 (2), 98–103 (in Chinese).
Zhao, J., Xi, X., Dong, H., et al., 2022. Rheo-microscopy in situ synchronous measurement of shearing thinning behaviors of waxy crude oil. Fuel 323, 124427. https://doi.org/10.1016/j.fuel.2022.124427.
Zhao, J., Li, X., Dong, H., et al., 2023. Rheo-optic in situ synchronous study on the gelation behaviour and mechanism of waxy crude oil emulsions. Pet. Sci. 20 (2), 1266–1288. https://doi.org/10.1016/j.petsci.2022.08.033.
Zhang, H., Cao, J., Duan, H., et al., 2022. Molecular dynamics insight into the adsorption and distribution of bitumen subfractions on Na-montmorillonite surface. Fuel 310, 122380. https://doi.org/10.1016/j.fuel.2021.122380.